arXiv:0908.3837v1 [nucl-th] 26 Aug 2009

Dynamical Model of Coherent Electroweak Pion Production Reactions on Nuclei

S. X. Nakamura*, T. Sato†, T.-S. H. Lee**, B. Szczerbinska‡ and K. Kubodera§

*Instituto de Física, Universidade de São Paulo, C.P. 66318, 05315-970, São Paulo, SP, Brazil
†Department of Physics, Osaka University, Toyonaka, Osaka, 560-0043, Japan
**Physics Division, Argonne National Laboratory, Argonne, Illinois 60439, USA
‡Dakota State University, College of Arts & Sciences, Madison, SD, 57042-1799, USA
§Department of Physics and Astronomy, University of South Carolina, Columbia, SC, 29208, USA

Abstract. We have developed a dynamical model for a unified description of the pion-nucleus scattering and photo- and neutrino-induced coherent pion production on nuclei. Our approach is based on a combined use of the Sato-Lee model for the electroweak pion production on a single nucleon and the Δ-hole model of pion-nucleus scattering. Numerical calculations are carried out for the case of the ^{12}C target. After testing our model with the use of the pion photo-production data, we confront our predictions of the neutrino-induced coherent pion production reactions with the recent data from K2K and MiniBooNE.

Keywords: neutrino-nucleus scattering, neutrino oscillation, pion production
PACS: 13.15.+g, 14.60.Pq, 25.30.Pt

INTRODUCTION

In recent years both the theoretical and experimental studies on the coherent pion production in neutrino-nucleus reactions in few-GeV region have been intense. These studies were originally inspired by the on-going and future neutrino experiments. Some interesting results from recent experiments have further encouraged the theoretical studies of this process. Namely, the K2K[1] and SciBooNE[2] collaborations reported no evidence of the charged-current (CC) process, while the MiniBooNE collaboration found a signal of the neutral-current (NC) process.[3] This discrepancy must be resolved since the isospin consideration predicts the simple relation $\sigma_{CC} \sim 2\sigma_{NC}$. The on-going data analysis of the coherent process have been trying to provide more detailed information including the muon and pion kinematics for the CC process, and some preliminary results have been presented in this workshop[4, 5]. Considering these experimental developments, it is important to develop a rigorous theoretical model for analyzing the available and the forthcoming data. This is the objective of our work.

There are mainly two types of theoretical approaches to the coherent pion production, i.e., a PCAC-based model and a microscopic model. We pursue the latter option. In a microscopic approach, the starting point is a model which can describe well the elementary electroweak pion production on a single nucleon in the considered energy region. Such a model has been developed by Sato and Lee[6] (SL) and is used in this work. The SL model also provides accurate pion-nucleon scattering amplitudes which are derived in a way consistent with the pion production amplitudes from the same Lagrangian. The πN scattering amplitudes are important ingredients in our calculations of an optical potential which describes the essential final pion-nucleus interactions. This optical potential takes account of the most important medium modifications of the Δ-propagation within the well-established Δ-hole model of pion-nucleus scattering. Therefore, a combined use of the SL model and the Δ-hole model, which seems promising for calculating pion production in nuclei, provide us with a consistent microscopic description of the pion scattering and the electroweak pion production mechanisms in nuclei. This consistency is an appealing point of our approach over the previous microscopic models for the coherent pion productions, and enables us to: (i) fix all free parameters in our model using the pion-nucleus scattering data; (ii) perform parameter-free calculations for the coherent pion productions; (iii) test the reliability of our approach using data for the photo-production process. Another important point to be noted is that we take care of the non-local effects on the in-medium Δ-propagation whose possibly large effect was pointed out recently [7]. For the neutrino-induced coherent pion production, no previous calculations (either in the PCAC-based or microscopic model) have included this effect.

Our calculations proceed as follows. We first employ the on- and off-shell πN scattering amplitudes generated from the SL model to construct a pion-nucleus optical potential within the Δ-hole model[8]. The parameters of the model are

determined by fitting the pion-nucleus scattering data. By using the pion-nucleus scattering wave functions generated from the constructed optical potential and the electroweak pion production amplitudes generated from the same SL model, we can calculate the coherent pion production cross sections. Our second step is to establish the reliability of our model by comparing the predicted pion photo-production cross sections with the available data. We then proceed to calculate the neutrino-induced coherent pion production cross sections. In the following sections, we explain our calculational framework, show some selected numerical results, and then conclude.

A DYNAMICAL MODEL

We briefly explain how we calculate the amplitude $A_{\lambda t\to\pi t}$ for the coherent pion production off a nucleus in its ground state (t) induced by an external current denoted by λ. Our starting point is a set of elementary amplitudes generated from the SL model, $a^{SL}_{\lambda N\to\pi N} = a_\Delta + a_{nr}$, where a_Δ (a_{nr}) denotes the resonant (non-resonant) part. The resonant part can be written as $a_\Delta = N/D(W)$, where $D(W) = W - m^0_\Delta - \Sigma(W)$ with W, m^0_Δ, Σ denoting the πN invariant mass, the bare Δ mass, and the Δ self energy, respectively. Within the Δ-hole model[8], we can include the medium effects by modifying the Δ propagator $D(W)$, and obtain the following expression of nuclear amplitude $A_{\lambda t\to\pi t}$

$$A_{\lambda t\to\pi t}(\boldsymbol{k},\boldsymbol{q}) \;=\; \sum_j \int \frac{d^3p_\Delta}{(2\pi)^3}\psi^*_j(\boldsymbol{p}'_N)\left[\frac{N(\tilde{\boldsymbol{k}},\tilde{\boldsymbol{q}})}{D(E+m_N-H_\Delta)-\Sigma_{\rm pauli}-\Sigma_{\rm spr}} + a_{nr}(\tilde{\boldsymbol{k}},\tilde{\boldsymbol{q}})\right]\psi_j(\boldsymbol{p}_N)\;, \tag{1}$$

where $\boldsymbol{q}$ and $\boldsymbol{k}$ ($\tilde{\boldsymbol{q}}$ and $\tilde{\boldsymbol{k}}$) are the momenta for the external current and the pion in the pion-nucleus (pion-nucleon) center-of-mass frame; $\boldsymbol{p}_\Delta = \boldsymbol{p}_N + \boldsymbol{q} = \boldsymbol{p}'_N + \boldsymbol{k}$. A single nucleon wave function in the initial [final] nucleus is denoted by $\psi_j(\boldsymbol{p}_N)$ [$\psi_j(\boldsymbol{p}'_N)$] with the index j specifying a nucleon orbit including the isospin state. The summation ($\sum_j$) is taken over the occupied states of the nucleus. The medium effects on the Δ-propagator are described by the Δ Hamiltonian (H_Δ), the Pauli-correction to the Δ self-energy ($\Sigma_{\rm pauli}$), and the so-called spreading potential ($\Sigma_{\rm spr}$). The spreading potential has the central and spin-orbit parts with their strengths determined by two free complex parameters in our model. The total energy of the pion-nucleus system is $E + Am_N$ (A: mass number). The integration over $\boldsymbol{p}_\Delta$ in Eq.(1) can be done analytically by fixing the $\boldsymbol{p}_\Delta$-dependence of the function in the square bracket to an effective constant value, except for the kinetic term in H_Δ which is is the source of the non-locality of the Δ propagation in nuclei. We then can sum over the nucleon states to obtain an expression which depends on the nuclear density; the nuclear density has been determined experimentally.

A full transition amplitude is obtained by convoluting the amplitude in Eq. (1) with the pion scattering waves. In this work, the pion scattering wave functions are obtained with an optical potential ($U_{\pi t}$). Our starting point of constructing $U_{\pi t}$ is the πN scattering amplitude generated from the SL model $T^{SL}_{\pi N} = t_\Delta + t_{nr}$, where t_Δ and t_{nr} are the resonant and non-resonant amplitudes, respectively. Consistently with Eq. (1), the Δ-propagator of the resonant part $t_\Delta = F_{\pi N\Delta}F_{\pi N\Delta}/D(W)$ is modified by the same procedure. The resulting optical potential is given by

$$U_{\pi t}(\boldsymbol{k}',\boldsymbol{k}) \;=\; \sum_j \int \frac{d^3p_\Delta}{(2\pi)^3}\psi^*_j(\boldsymbol{p}'_N)\left[\frac{F_{\pi N\Delta}(\tilde{\boldsymbol{k}}')F_{\pi N\Delta}(\tilde{\boldsymbol{k}})}{D(E+m_N-H_\Delta)-\Sigma_{\rm pauli}-\Sigma_{\rm spr}} + t_{nr}(\tilde{\boldsymbol{k}}',\tilde{\boldsymbol{k}})\right]\psi_j(\boldsymbol{p}_N) + c\rho^2\;. \tag{2}$$

The last term of the above expression is a phenomenological term proportional to the square of the nuclear density. It describes the absorption of s- and p-wave pions by a pair of nucleons and hence is determined by two complex couplings c_s and c_p. Thus we have four free parameters in our model: c_s and c_p, and two parameters specifying the strength of the spreading potential which are needed to calculate $\Sigma_{\rm spr}$ in Eqs.(1)-(2). We determine these four parameters by fitting to the pion-nucleus scattering data. We then can perform parameter-free calculations of the coherent electroweak pion production cross sections.

RESULTS

Pion-nucleus scattering

We determine the four free parameters of our model by fitting to the available pion-nucleus scattering data in the 50 MeV $\lesssim T_\pi \lesssim$ 300 MeV region. (T_π is the pion kinetic energy in the laboratory frame.) Two sample results from

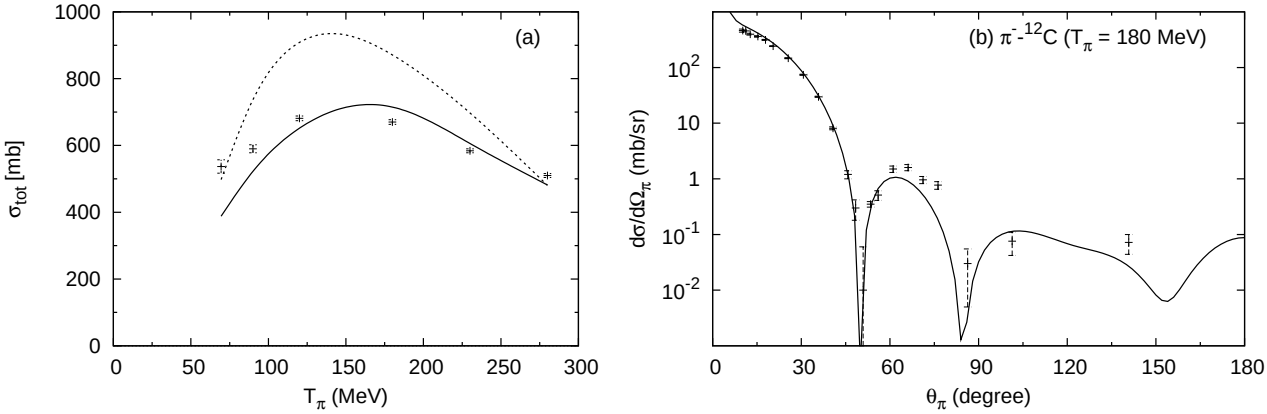

FIGURE 1. (a) Total cross sections for $\pi^- - {}^{12}$C scattering. The solid curve is obtained with our full calculation, while the dashed curve is obtained without the spreading potential. (b) $\pi^- - {}^{12}$C elastic differential cross sections at T_π = 180 MeV. The solid curve is obtained with our full calculation. In both figures, the data are from Ref. [9].

our fits to the $\pi - {}^{12}$C scattering data are shown in Fig. 1. In the left-hand side of Fig. 1, we see that the total cross sections for π^--^{12}C scattering as a function of T_π can be reproduced very well by our full calculations (solid curve). For a comparison, the results obtained without including the spreading potential are shown in the dashed curve. We observe a large reduction from the dashed to solid curves, indicating the importance of the strong pion absorption simulated by the spreading potential. In the right hand side of Fig. 1, we see that our model can also describe very well the differential cross sections. Overall, our model can satisfactorily reproduce the data for both the total and elastic cross sections in the considered 50 MeV $\lesssim T_\pi \lesssim$ 300 MeV energy region.

With the four parameters of our model determined in the fits to the pion-nucleus scattering, we are now in a position to perform parameter-free calculations of the coherent electroweak pion production cross sections.

Coherent pion photo-production

The photo-production process, for which extensive data are available, provides a good testing ground for our approach. In the left-hand-side of Fig. 2 we compare the existing data with our results for the differential cross sections of $\gamma + {}^{12}\mathrm{C}_{g.s.} \to \pi^0 + {}^{12}\mathrm{C}_{g.s.}$. The solid curve is the result of our full calculation. The long-dashed curve is obtained without including the pion-nucleus final state interaction (FSI) and without including the the medium effects ($\Sigma_{\rm pauli}$ and $\Sigma_{\rm spr}$) on the Δ-propagation of Eq.(1). When the the medium effects on the Δ propagation in Eq.(1) is included, we obtain the short-dash curve. By comparing these three curves, it is clear that the medium effects are quite sizable, and they play an important role in bringing the calculated differential cross sections in agreement with the data. The good general agreement seen in Fig. 2(a) indicates the basic soundness of the method we have used in determining the spreading potential. It is true that, in the relatively larger angle region, there are noticeable discrepancies between the results of our full calculation and the data. We remark however that, as noted in Ref. [10], the data in this region are likely to be substantially contaminated by incoherent processes in which the final nucleus is in its low-lying excited states.

As a comparison, the dash-dotted curve in left hand side of Figure 2 is obtained when the non-resonant pion production amplitude[1] is set to zero. Clearly, the non-resonant production is substantial and can not be neglected. In general, we observe that, even near the resonance energy, the contribution from the non-resonant mechanism is quite significant. This is partly because the resonant contribution is considerably suppressed by pion absorption (the spreading potential) and the non-local effect of Δ propagation (Δ kinetic term).

Through the comparison of our numerical results with the pion photo-production data, we have established the

[1] In the SL model, the resonant amplitude itself contains the non-resonant mechanisms. We refer to purely non-resonant amplitudes as "non-resonant amplitudes".

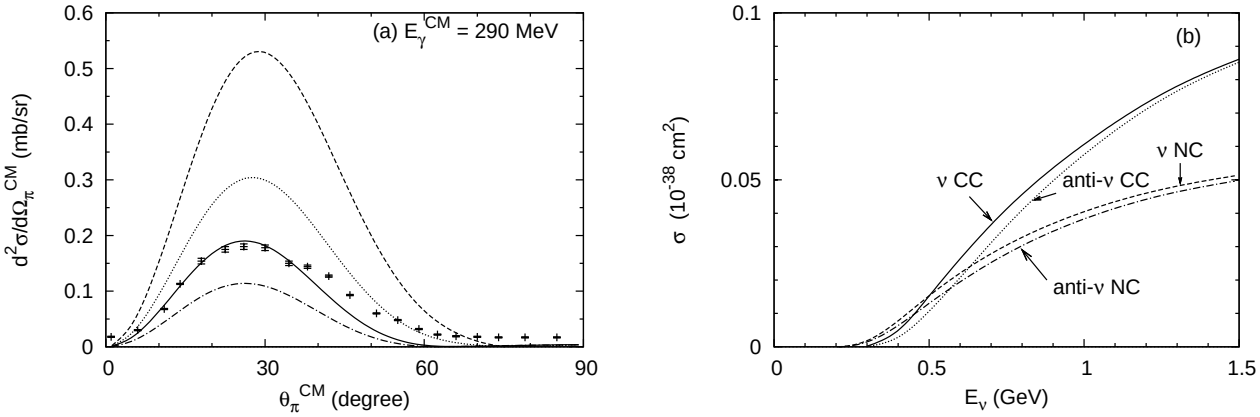

FIGURE 2. (a) Differential cross sections for $\gamma + {}^{12}\mathrm{C}_{g.s.} \to \pi^0 + {}^{12}\mathrm{C}_{g.s.}$. The solid line represents the result of the full calculation. The long-dashed line is obtained without the FSI and without the medium effects on the Δ-propagation, while the short-dash line is obtained with the medium effects on the Δ included. The dash-dotted line corresponds to a case in which the pion production operator includes only the Δ mechanism. The data are from Ref. [10]. (b) The E_ν-dependence of the total cross section for $\nu_\mu + {}^{12}\mathrm{C}_{g.s.} \to \mu^- + \pi^+ + {}^{12}\mathrm{C}_{g.s.}$ (solid line), $\nu + {}^{12}\mathrm{C}_{g.s.} \to \nu + \pi^0 + {}^{12}\mathrm{C}_{g.s.}$ (dashed line), $\bar{\nu}_\mu + {}^{12}\mathrm{C}_{g.s.} \to \mu^+ + \pi^- + {}^{12}\mathrm{C}_{g.s.}$ (dotted line) and $\bar{\nu} + {}^{12}\mathrm{C}_{g.s.} \to \bar{\nu} + \pi^0 + {}^{12}\mathrm{C}_{g.s.}$ (dash-dotted line).

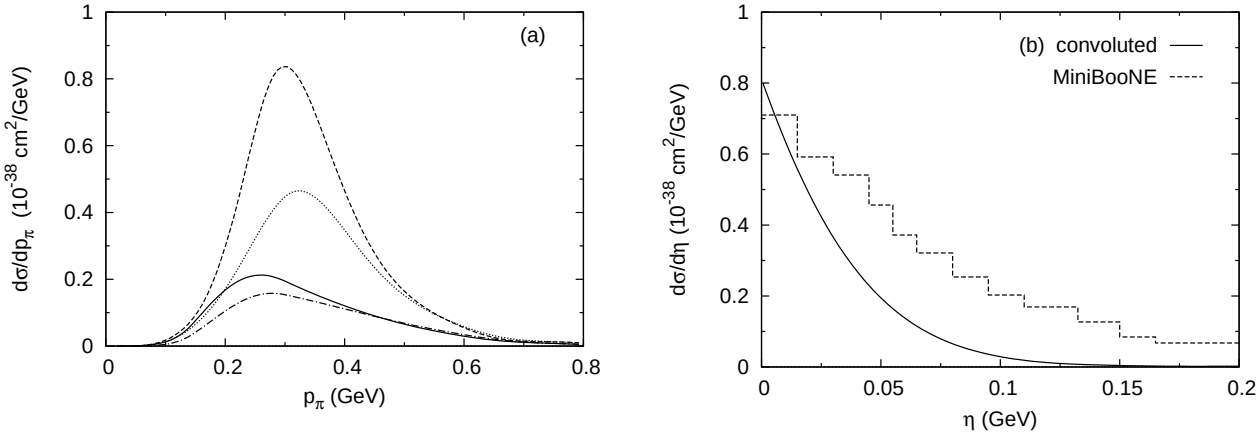

FIGURE 3. (a) The pion momentum distribution for $\nu_\mu + {}^{12}\mathrm{C}_{g.s.} \to \mu^- + \pi^+ + {}^{12}\mathrm{C}_{g.s.}$ at E_ν = 1 GeV; p_π is the pion momentum in the laboratory frame. The use of the solid, dashed, dotted and dash-dotted lines follows the same convention as in Fig. 2(a). (b) The flux-convoluted η-distribution for $\nu + {}^{12}\mathrm{C}_{g.s.} \to \nu + \pi^0 + {}^{12}\mathrm{C}_{g.s.}$ obtained in our full calculation. The neutrino flux is taken from MiniBooNE [11]. Also shown is the Monte Carlo result from MiniBooNE [3] rescaled.

reliability of our approach based on a combined use of the SL model and the Δ-hole model. Thus we proceed to apply the same approach to make predictions for cross sections of the neutrino-induced coherent pion production on ^{12}C.

Neutrino-induced coherent pion production

We now present our predictions of the neutrino-induced coherent pion production on the ^{12}C target. We consider the CC and NC processes induced by a neutrino or an anti-neutrino. In the right-hand-side of Figure 2. we show the predicted total cross sections for these processes as functions of the incident neutrino (anti-neutrino) energy E_ν in the laboratory system. It is seen that, for higher incident energies, the ratio σ_{CC}/σ_{NC} approaches 2, a value expected from the isospin factor. For lower incident energies ($E_\nu \lesssim 500$ MeV), however, σ_{NC} is larger than σ_{CC}, reflecting the fact that the phase space for the CC process is reduced significantly by the muon mass. To compare our results

with data, we need to evaluate the total cross sections averaged over the neutrino fluxes that pertain to the relevant experiments. We choose to use the fluxes up to $E_\nu \leq 2$ GeV and neglect the fluxes beyond that limit. We also need to consider the experimental setting such as kinematical cuts. A K2K experiment [1] reports the upper limit for the neutrino CC coherent pion production, $\sigma_{\rm K2K} < 7.7 \times 10^{-40}{\rm cm}^2$. This upper limit corresponds to events satisfying the muon momentum cut, $p_\mu > 450$ MeV and the cut on the square of the momentum transfer, $Q^2_{\rm rec} < 0.1$ GeV^2; $Q_{\rm rec}$ is the momentum transfer reconstructed with an assumption of the quasi-free kinematics. Therefore, we also calculate the total cross section with these cuts and then convolute with the flux reported by the K2K experiment [12]. We obtain $\sigma^{CC}_{\rm ave} = 6.3 \times 10^{-40}{\rm cm}^2$ which is consistent with the upper limit from K2K.

For the NC process, we use the flux reported by MiniBooNE in Ref. [11] and arrive at $\sigma^{NC}_{\rm ave} = 2.8 \times 10^{-40}{\rm cm}^2$; no kinematical cut is necessary in this case. This is to be compared with $\sigma_{\rm MiniBooNE} = 7.7 \pm 1.6 \pm 3.6 \times 10^{-40}{\rm cm}^2$ given in Ref. [13]. Our result is consistent with the empirical value within the large experimental errors, even though the theoretical value is rather visibly smaller than the empirical central value. It is to be noted however that Ref. [13] is a preliminary report, and that, as discussed in great detail in Ref. [14], $\sigma_{\rm MiniBooNE}$ may be overestimated due to the use of the Rein-Sehgal (RS) model[15] in the analysis.

Next, we present our result for the pion momentum spectrum for the CC process at E_ν = 1 GeV in Fig. 3(a). The importance of the medium effects itself here in the same manner as in the photo-process [Fig. 2(a)]. In the Δ region, strong pion absorption is seen to reduce the cross sections significantly, and FSI shifts the peak position. The dash-dotted line corresponds to a case in which the pion production operator contains only the Δ mechanism (without non-resonant contributions), while the pion optical potential is kept unchanged. We note that, at E_ν = 1 GeV, the dash-dotted line corresponds to 82% of the solid line, and for E_ν = 0.5 GeV, 64%. The result indicates that the non-resonant components in our model play a significant role in the coherent pion production; their role is particularly important for $E_\nu \lesssim 0.5$ GeV. This characteristic feature of our model should be contrasted with the fact that non-resonant mechanisms play essentially no role in any of the previous microscopic calculations for neutrino-induced coherent pion production.

We examine the effects of the non-locality of Δ-propagation in nuclei arising from the Δ kinetic term. For this purpose, we introduce a quantity $\mathscr{R}(E_\nu) \equiv \sigma(E_\nu)/\sigma_{\rm local}(E_\nu)$, where σ ($\sigma_{\rm local}$) is calculated with (without) the Δ kinetic term. This subject has been studied in Ref. [7] which included the Δ-mechanism only, without FSI or medium modifications of the Δ. They showed that the cross section is changed by $\mathscr{R} \lesssim 0.5, \sim 0.6, \lesssim 1$ at E_ν = 0.5, 1, 1.5 GeV. When we use the free Δ-propagator without FSI, which contains the physics similar to that of Ref. [7], we find that the non-locality change the cross sections by $\mathscr{R} = 0.41, 0.74, 0.88$ at E_ν = 0.5, 1, 1.5 GeV. This result is fairly close to that obtained in Ref. [7]. Next we use the Δ-propagator in Eq. (1) but without the major medium effects ($\Sigma_{\rm spr}$, $\Sigma_{\rm pauli}$, and small effects), and then find that the effect of the non-locality is somewhat moderated: $\mathscr{R} = 0.54, 1.03$ and 1.14 at E_ν = 0.5, 1.0 and 1.5 GeV. Including the non-resonant amplitudes, medium effects on the Δ and FSI, the effect of the non-locality is $\mathscr{R} = 0.34, 0.73, 0.84$ at E_ν = 0.5, 1, 1.5 GeV for the full calculation, showing that the non-locality is still important. Even though the non-locality might be partly accounted for with the use of the spreading potential fitted to data, considering its importance, it is preferable to take it into account explicitly.

The MiniBooNE analysis of NC data used the η-distribution [$\eta \equiv E_\pi(1-\cos\theta_\pi)$] to distinguish coherent pion production from the other processes contributing to the π^0-production events. To this end, MiniBooNE used the "shape" of the η-distribution obtained from the RS model [15] with the momentum reweighting function applied. However, a microscopic calculation in Ref. [14] was found to give an η-distribution appreciably different from that obtained in the RS model, and the authors of Ref. [14] pointed out a possibility that the MiniBooNE might have substantially overestimated the NC events. Thus it is interesting to compare our result with the η-distribution from MiniBooNE. Figure 3(b) shows the "average" η-distribution, resulting from the convoluting of the η-distribution obtained in our present calculation with the MiniBooNE neutrino flux [11]. The figure also presents the MiniBooNE Monte Carlo results (*cf.* Fig. 3b of Ref. [3]), arbitrarily rescaled to match the theoretical curve at η = 0.005 GeV. We remark that the η-distribution we have obtained is fairly close to that given in Ref. [14]. and thus also arrive at the conclusion that it is possible that MiniBooNE might have substantially overestimated the NC events.

DISCUSSION AND SUMMARY

Recent theoretical efforts on the neutrino-induced coherent pion production are indeed active, and it is interesting to see a numerical comparison of those calculations. Such a comparison has been presented at this conference[16]. Because of the lack of data, it is impossible to rate the models from the comparison. In the following, however, we argue that our present calculation would have advantages over the existing calculations. Our model provides, thanks

to the consistency built in the SL model, a consistent description of the pion-nucleus scattering and the photo- or neutrino-induced coherent pion productions. Because of the consistency, we were able to fix the parameters using the data for the pion-nucleus scattering and to predict the coherent processes. It is also the consistency which enables us to test our approach using the existing data for the photo-process. No other microscopic calculation for the neutrino-induced coherent pion production has been checked to this level. Besides, all the other previous calculations lack the non-locality of Δ-propagation whose importance was examined in the previous section. Further remark is concerned with FSI. Our optical potential is made to reproduce the data for the pion-nucleus scattering in the range of 50 MeV $\lesssim T_\pi \lesssim$ 300 MeV, covering the most important Δ region. On the other hand, in the other microscopic calculations, their optical potential may not be as accurate as ours. For example, let us look into the model of Amaro et al. [14], which is the most sophisticated among the existing microscopic models for neutrino-induced coherent pion production. The parameters in their optical potential were fitted to the data for the binding energies of pionic atoms. Because, in the present context, the optical potential should work well over relatively wide energy region around the Δ region, the optical potential used in Ref. [14] may contain a questionable aspect. Finally we mention that it has become fairly clear that the RS model, the prominent PCAC-based model, does not work reasonably for $E_\nu \lesssim 2$ GeV. This point was made clear through the detailed study of the relation between the RS model and the microscopic model in Ref. [14]. Although some improvements on the RS model has been proposed[17, 18, 19], the applicability of a PCAC-based model to the relevant energy region is currently a subject of controversy.

In summary, we have developed a microscopic model based on a combination of the SL and the Δ-hole models. The model provides a consistent description of the pion-nucleus scattering and the coherent pion production processes. Utilizing the consistency, we can fix the free parameters in our model using the pion-nucleus scattering data, and then give parameter-free predictions for the coherent processes. After testing the reliability of our approach using the data for the photo-process, we calculate and present results for the neutrino-induced coherent pion production.

ACKNOWLEDGMENTS

This work is supported by the Natural Sciences and Engineering Research Council of Canada and Universidade de São Paulo (SXN), by the U.S. Department of Energy, Office of Nuclear Physics, under contract DE-AC02-06CH11357 (TSHL), by the Japan Society for the Promotion of Science, Grant-in-Aid for Scientific Research(C) 20540270 (TS), and by the U.S. National Science Foundation under contract PHY-0758114 (KK).

REFERENCES

1. M. Hasegawa et al. [K2K Collaboration], *Phys. Rev. Lett.* **95**, 252301 (2005).
2. K. Hiraide et al. [SciBooNE Collaboration], *Phys. Rev. D* **78**, 112004 (2008).
3. A. A. Aguilar-Arevalo et al. [MiniBooNE Collaboration], *Phys. Lett. B* **664**, 41 (2008).
4. K. Hiraide, in these proceedings of NUINT09.
5. H. Tanaka, in these proceedings of NUINT09.
6. T. Sato and T.-S. H. Lee, *Phys. Rev. C* **54**, 2660 (1996); T. Sato, D. Uno and T.-S. H. Lee, *Phys. Rev. C* **67**, 065201 (2003).
7. T. Leitner, U. Mosel, S. Winkelmann, *Phys. Rev. C* **79**, 057601 (2009).
8. B. Karaoglu and E. J. Moniz, *Phys. Rev. C* **33**, 974 (1986).
9. F. Binon, et al., *Nucl. Phys.* **B17**, 168 (1970).
10. B. Krusche et al., *Phys. Lett. B* **526**, 287 (2002).
11. A.A. Aguilar-Arevalo et al. [MiniBooNE Collaboration], *Phys. Rev. D* **79**, 072002 (2009).
12. M. H. Ahn et al., *Phys. Rev. D* **74**, 072003 (2006).
13. J. L. Raaf, PhD thesis, University of Cincinnati, FERMILAB-THESIS-2007-20 (2005).
14. J.E. Amaro, E. Hernandez, J. Nieves and M. Valverde, *Phys. Rev. D* **79**, 013002 (2009).
15. D. Rein, L. M. Sehgal, *Nucl. Phys.* **B223**, 29 (1983).
16. S. Dytman et al., in these proceedings of NUINT09.
17. Ch. Berger and L.M. Sehgal, *Phys. Rev. D* **79**, 053003 (2009).
18. E. A. Paschos, A. Kartavtsev and G.J. Gounaris, *Phys. Rev. D* **74**, 054007 (2006).
19. E. Hernández, J. Nieves, M.J. Vicente-Vacas, *Phys. Rev. D* **80**, 013003 (2009).